Laser and Particle Beams (2004), *22*, 461–467. Printed in the USA.

DOI: 10.1017/S0263034604040108

A study of the parameters of particles ejected from a laser plasma

D. DORIA,[1,2] A. LORUSSO,[1,2] F. BELLONI,[1,2] V. NASSISI,[1,2] L. TORRISI,[3,4] AND S. GAMMINO[4]

[1]Department of Physics of Lecce, Laboratorio di Elettronica Applicata e Strumentazione, Lecce, Italy
[2]INFN sez. di Lecce, Lecce, Italy
[3]Department of Physics of Messina, Lecce, Italy
[4]INFN, Laboratori Nazionali del Sud, Catania, Italy

(RECEIVED 17 February 2004; ACCEPTED 16 July 2004)

Abstract

We report on the results concerning the characteristics and the behavior of expanding plasma generated by a Laser Ion Source (LIS). The LIS technique is an efficient means in producing of multi-charged ions utilizing pulsed laser beams. In order to extract Cu ions, in this experiment an XeCl excimer UV laser was employed, providing a power density on the target surface up to 5×10^8 W/cm^2. Two typologies of diagnostic systems were developed in order to detect the plasma current and the ion energy. The time-of-flight (TOF) measurements were performed exploiting either a Faraday cup or an Ion Energy Analyzer (IEA). This latter allowed getting quantitative information about the relative ion abundances, their kinetic energy and their charge state. To study the plasma characteristics we measured the total etched material per pulse at 70 mJ. It was 0.235 μg and the overall degree of ionization, 16%. The angular distribution of the ablated material was monitored by optical transmission analysis of the deposited film as a function of the angle with respect to the normal to the target surface. Applying a high voltage to an extraction gap a multi-charged ion beam was obtained; different peaks could be distinguished in the TOF spectrum, resulting from the separation of ions of hydrogen, adsorbed compounds in the target and copper.

Keywords: Ion energy analyzer; Laser ion source; Laser plasma

1. INTRODUCTION

A lot of new applications with ion beams, not only in research laboratories (Ciavola & Gammino, 1992), but also in the fields of industry, engineering and hadrontherapy (Picardi *et al*., 1994), have stimulated great interest in new ion sources. The new applications need ion beams of low energy spread and good geometric quality. These ion beam characteristics can be got utilizing no conventional techniques, such as high energy electron beams or high frequency resonance, or simply exploiting the interaction of laser beams of high pulsed energy with the matter (Henkelmann *et al*., 1992; Luches *et al*., 1993).

Laser beams of high pulse intensity allow the production of etched material acting directly on solid target without the application of special devices for evaporation. The laser interaction produces an exploding plasma plume consisting of high concentration ionized matter, which in turn can generate high ion beam current of short duration. The plasma evolves mainly in the perpendicular direction to the target surface, so advantaging the application of accelerating electrodes and then the formation of ion beams. Such beams are very interesting for injecting ions into large accelerators (Dubenkov *et al*., 1996; Sharkov *et al*., 1998; Kondrashev *et al*., 2000).

Laser-matter interaction technique is also used to generate plasma for pulsed laser deposition (PLD) of thin films, as well as to get morphological changes of a large variety of polymers in order to improve their stoichiometry, adhesion and wetting (Wong *et al*., 2003). For these goals many studies have been carried out in order to predict the plasma gas-dynamics and the PLD film properties (Anisimov *et al*., 1993) considering the generated gas fairly neutral. Really, in these experiments the percentage of charged particles is not negligible as well as their angular distribution and temporal evolution. These characteristics influence the deposition quality of PLD films. Therefore, an accurate diagnostics of the plasma is potentially useful in order to improve the quality of both ion beams and deposited films.

Address correspondence and reprint requests to: F. Belloni, Department of Physics, Laboratorio di Elettronica Applicata e Strumentazione (LEAS), 73100 Lecce, Italy. E-mail: fabio.belloni@le.infn.it

A laser beam incident on a solid target causes evaporation of some material layers and, due to the energy absorbed via electron-ion inverse Bremsstrahlung, ions are generated (Sherwood, 1992; Henkelmann *et al.*, 1992). The evaporating material interacts with the laser beam all through its duration, obtaining a progressive ionization of the plasma. In this stage soft X-rays also are generated.

In these experiments the initial plasma can reach temperatures of hundreds of eV (Kruer, 1986). These energy values are greater than those necessary to ionize the atoms of the target material. The interaction even produces electrons, atoms, molecules, clusters and ions. Experiments have put in evidence the generation, from many materials, of multiple charge state ions with energies up to thousands of keV (Làska *et al*., 2000). For such energies, it is clear that during the plasma expansion, the plume particles can enhance the source yield producing new ions. In these experiments the laser wavelength plays an important role. Generally, IR lasers enhance the charge state, while UV lasers enhance the current value (Torrisi *et al*., 2003).

In this work, we present experimental results obtained by a short wavelength excimer laser of relatively low intensity. Preliminary results on beam extraction are also reported.

2. EXPERIMENTAL APPARATUS AND RESULTS

We utilized a pulsed XeCl excimer laser (λ = 308 nm) having a 20 ns pulse width able to deposit on the target a maximum energy of about 100 mJ, reaching a laser power of 5 MW. The apparatus utilized in this experiment was very versatile and could be arranged in different configurations. It is shown in Figure 1 and consisted of a vacuum generating chamber (GC), 30 cm long, and a drift tube (DT), 124 cm long. In order to focalize the laser beam on the target, we used a convergent lens (15 cm focal length) together with a set of neutral density filters to modify the pulse energy. The angle between the normal to the target surface and the laser beam was 70°. The target support was a stem mounted on the generating chamber by an insulating (I) connector. This arrangement presents the advantage to apply an accelerating voltage directly to the target, keeping the chamber and the vacuum system to ground. The experimental set-up was completed by an 18 cm long removable expansion chamber connected mechanically and electrically to the target, which allowed the ions contained in the plasma to get an initial free expansion, Figure 2. A ground electrode in front of the expansion chamber allowed generating an intense electric field which accelerated the charged particles.

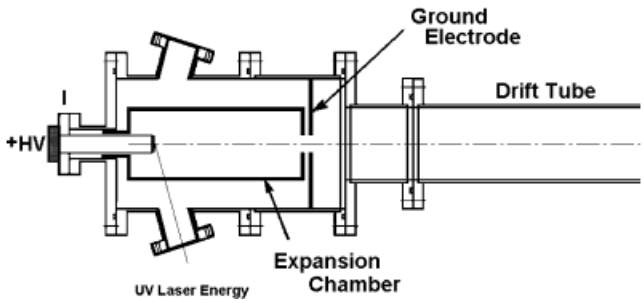

Fig. 2. Sketch of the generating chamber containing the accelerating system.

The diagnostic systems consisted of an electrostatic mass spectrometer and an ion collector. The former is a cylindrical electrostatic ion energy analyzer (IEA) which allowed us to discriminate ions of a certain charge-to-mass ratio and kinetic energy, while the latter was an aluminum coaxial Faraday cup (FC), 8 cm in diameter, closed on a 50 Ω load resistor by a transmission line and a 5 μF capacitor, Figure 3. The FC was equipped with a suppression ring in order to avoid secondary electron emission from the collector.

To estimate the size of the ablated surface we analyzed the profile of the laser beam on the lens focal plane by a joule-meter and a movable straight-edge. By finely translating the straight-edge with a step of 0.05 mm we obtained the experimental data concerning the spatial integral in two dimensions of the laser beam intensity profile. Supposing the laser beam profile to be gaussian, we fitted the experimental data with a suitable *erf* function. Figure 4 shows the gaussian intensity profile obtained as described above and taking into account that the laser direction is tilted of 70° with respect to the chamber axis. Since the fluence threshold value to get Cu ablation is 0.7 J/cm^2, the area of the laser

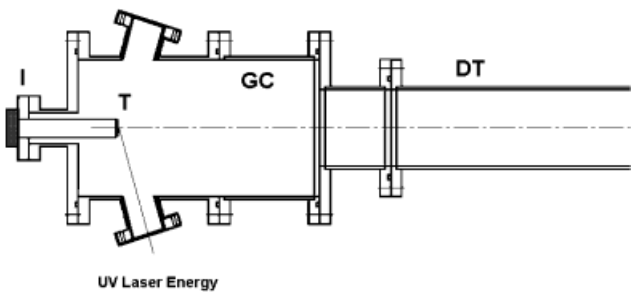

Fig. 1. Experimental apparatus. GC: Generating Chamber, DT: Drift Tube, T: Target, I: target Insulator.

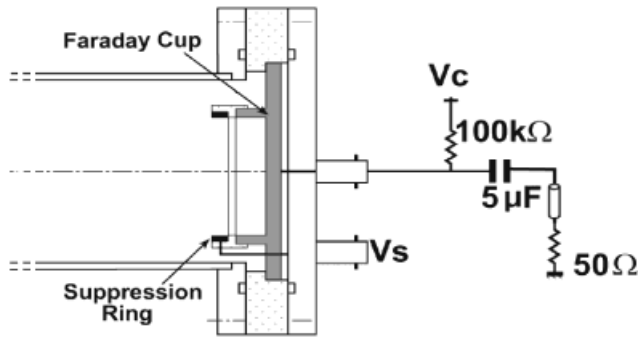

Fig. 3. Sketch of the Faraday cup. V_c: Faraday cup polarization voltage; V_s: suppressor ring polarization voltage.

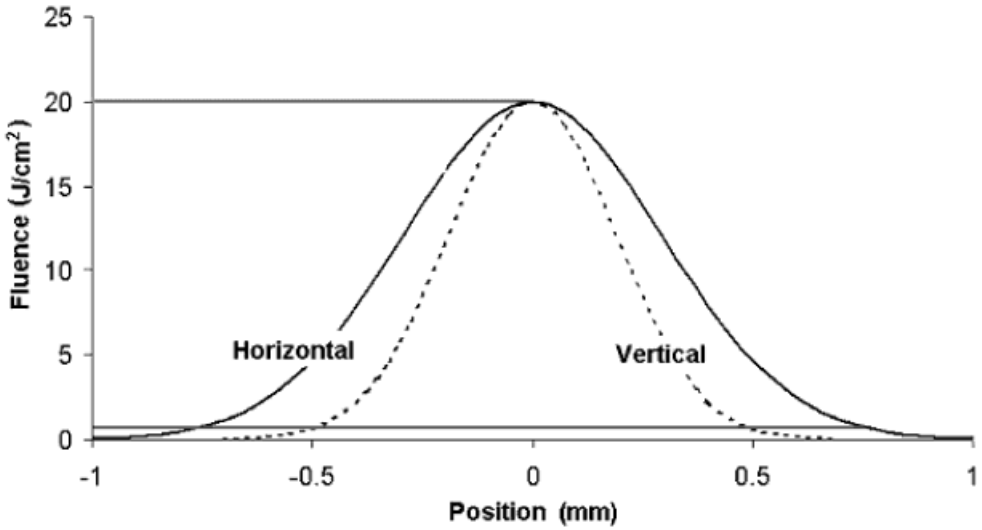

Fig. 4. Laser spot energy density on horizontal direction (70° tilted with respect to the laser axis) and vertical direction.

spot resulted equal to about 1 mm^2. Therefore the laser power density was estimated 3.5×10^8 W/cm^2 at working laser energy of 70 mJ.

2.1. Plasma characteristics

At about 2 cm from the target we placed a glass substrate in order to evaluate the angular distribution of the ejected particles by the deposited material thickness. During the deposition the target was continuously rotated in order to avoid the plasma flux deviation due to the progressive modification of the irradiated surface morphology. The film thickness distribution was determined by measuring its optical transmittance by a He-Ne laser as light source and an IR photodiode as detector. The deposited film was inserted between laser and photodiode and translated. To assess the film profile a 0.2 mm pinhole was placed in front of the detector. The input (I_{in}) and output (I_{out}) intensities are linked by the well known absorption relation

$$I_{out} = I_{in} e^{-\alpha x} \tag{1}$$

where x is the film thickness and α is the absorption coefficient (6.85×10^5 cm^{-1}) of the deposited film at He-Ne wavelength. The ablated material profile we obtained is shown in Figure 5 as a function of the angle. As it can be seen, the ejected material has a symmetric distribution and a narrow directionality (FWHM = 45°), that is very interesting for the coupling between LIS and accelerators. According to a well established habit, we fitted the experimental profile with a function of the form $cos^n(\theta)$, obtaining $n \approx 10$, in agreement with data previously reported in literature.

In these conditions the ablated material quantity, containing both neutral and charged particles, was estimated by measuring the mass of the target before and after the laser irradiation by means of a highly sensitive digital balance (Sartorius ME215S). Due to the low yield of ejected material per pulse, the laser irradiation consisted of 2000 laser pulses. The ablation rate we found was 0.235 μg/pulse, which corresponded to 2.2×10^{15} ejected atoms per pulse.

As suggested in the introduction, during the plasma propagation the fastest particles can contribute to enhance the ionization degree, but also the recombination. With our cup we were able to perform measurements of the plasma current along the propagation tube. The FC, with a bias voltage of -100 V, was placed at 20 cm from the target and the laser energy was fixed at 70 mJ. With such a set-up configuration we were able to appraise the charge yield. For these kinds of measurements the cup suppressor electrode resulted unnecessary because of the moderate energy of the particles contained in the free expanding plasma. By the experimental angular distribution of the ejected material shown in Figure 5, we calculated that the cup, 8 cm in diameter, could collect the whole ejected particles only at distances from the target lower than about 6 cm. But at low distances from the target, the cup voltage and the high plasma density generated arcs, so we were not able to perform measurements of the real plasma current. So, we recorded the plasma current at a target-cup distance of about 20 cm with a working laser fluence of 7 J/cm^2. Considering the angular distribution of ejected material, at such a distance we collected only the 20% of the whole number of ablated particles because the solid angle is restricted to only 0.12 sr. Now, taking into account the angular distribution of the ejected particles, we obtained that the produced total charge is 87 μC.

2.2. Energy distribution of the produced ions

The energy of the produced ions plays an important role for the PLD quality and for the ion injection in accelerator. The distribution of ion energy can be easily found by utilizing the IEA instrument (Fig. 6). It consists of two baffle-plates

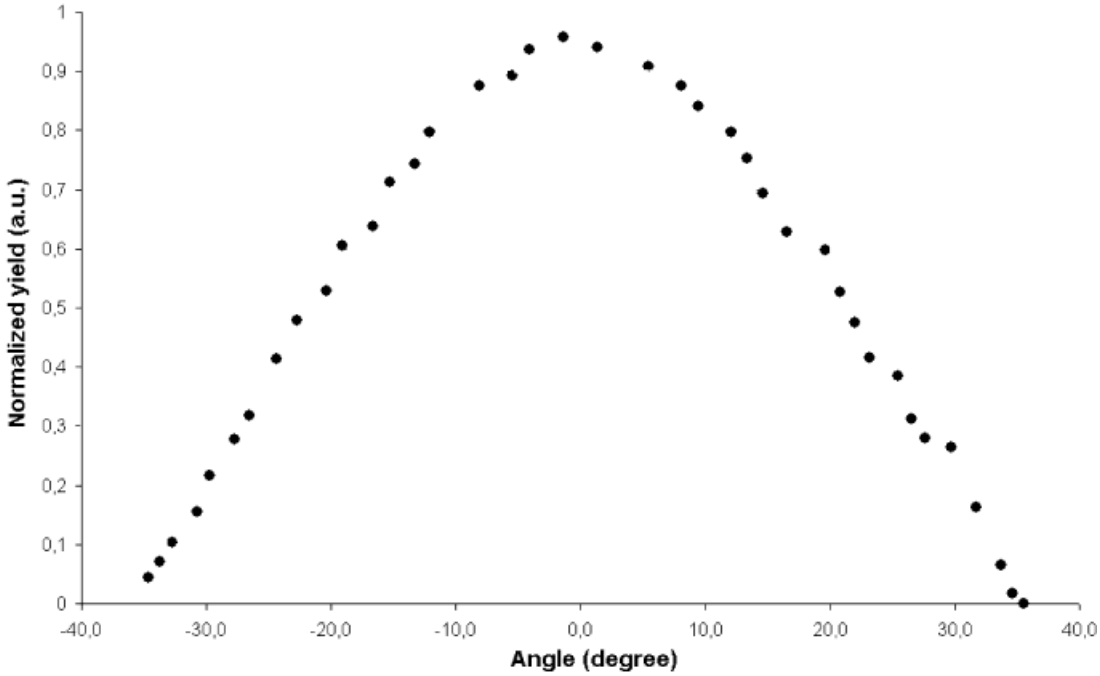

Fig. 5. Angular profile of the ablated material (FWHM = 45°).

electrostatically charged and a windowless electron multiplier (WEM). The voltages of the two baffle-plates are equal and opposite, $V_1 = -V_0$ and $V_2 = V_0 > 0$, and V_0 is changed to obtain a selection of the ion mass-to-charge ratio (m/ze). The TOF value of the ions able to pass the IEA filter is given by the following equation:

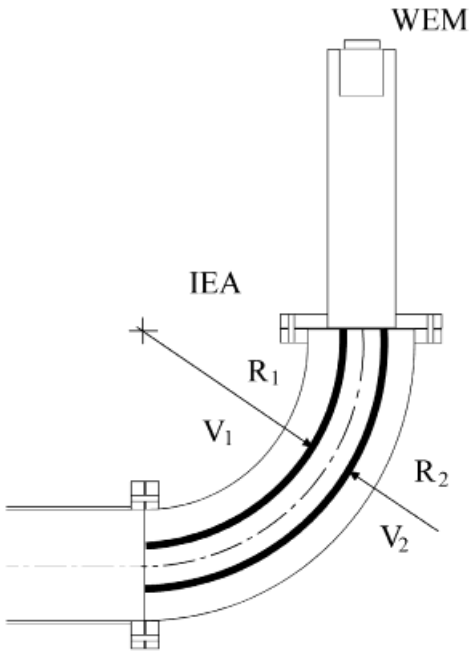

Fig. 6. Sketch of the Ion Energy Analyzer (IEA). R_1 and R_2: electrode radii; V_1 and V_2: electrode voltages.

$$TOF = L\sqrt{\frac{m/ze}{2\gamma V_0}} \tag{2}$$

where L is the distance between the target and the WEM ($L = 2$ m), γ is a constant depending on the system geometry ($\gamma = 20$), m is the ion mass ($m = 63.55$ amu), z and e are the charge state and the electron charge, respectively. Therefore, the energy of the particles reaching the WEM is:

$$E = \gamma z e V_0. \tag{3}$$

A typical IEA signal displaying the Cu^{+1}, Cu^{+2}, Cu^{+3}, Cu^{+4}, and Cu^{+5}/C^{+1} peak at $V_0 = 30$ V is shown in Figure 7. To test the reliability of IEA we performed measurements of the only Cu^{+1} peak. By this way we were able to distinguish the isotope composition of the copper. Figure 8 shows the two Cu isotope peaks ($Cu^{63} = 69.2\%$ and $Cu^{65} = 30.8\%$).

To better understand the ion formation, we found the copper ion distribution for different charge states and several laser energies. The obtained data give us information about the relative abundance and the energy distribution of the ions at fixed laser energy, as reported in Figure 9. As one can note, at 70 mJ laser energy, 50% of ions are single ionized and roughly the other 50% is double ionized; so, taking into account the data in the above paragraph, the overall degree of ionization results about 16%. This is a high percentage that makes this apparatus very interesting.

To determine plasma temperature and drift velocity we assumed a shifted Maxwell-Boltzmann distribution for the ion velocity (Kelly, 1990), obtaining the Eq. 4 for the IEA signal:

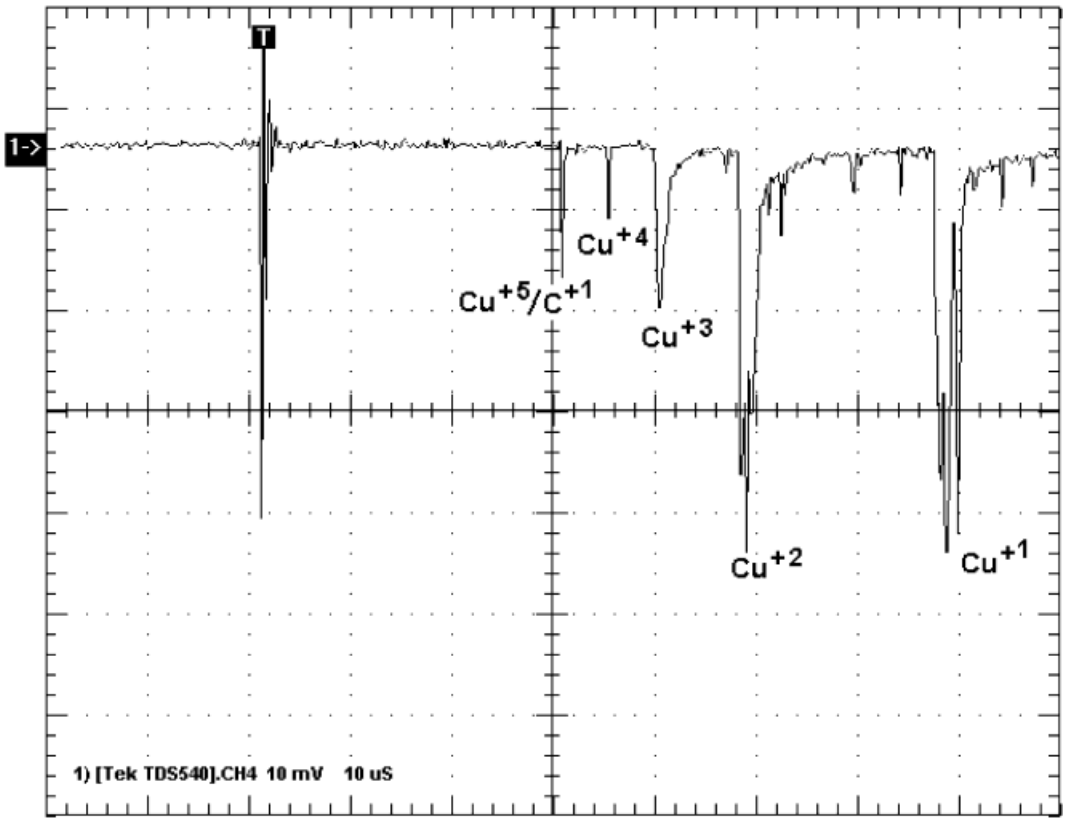

Fig. 7. Typical IEA signal showing the Cu^{+1}, Cu^{+2}, Cu^{+3}, Cu^{+4}, and Cu^{+5}/C^{+1} peaks at $V_0 = 30$ V and 70 mJ laser energy.

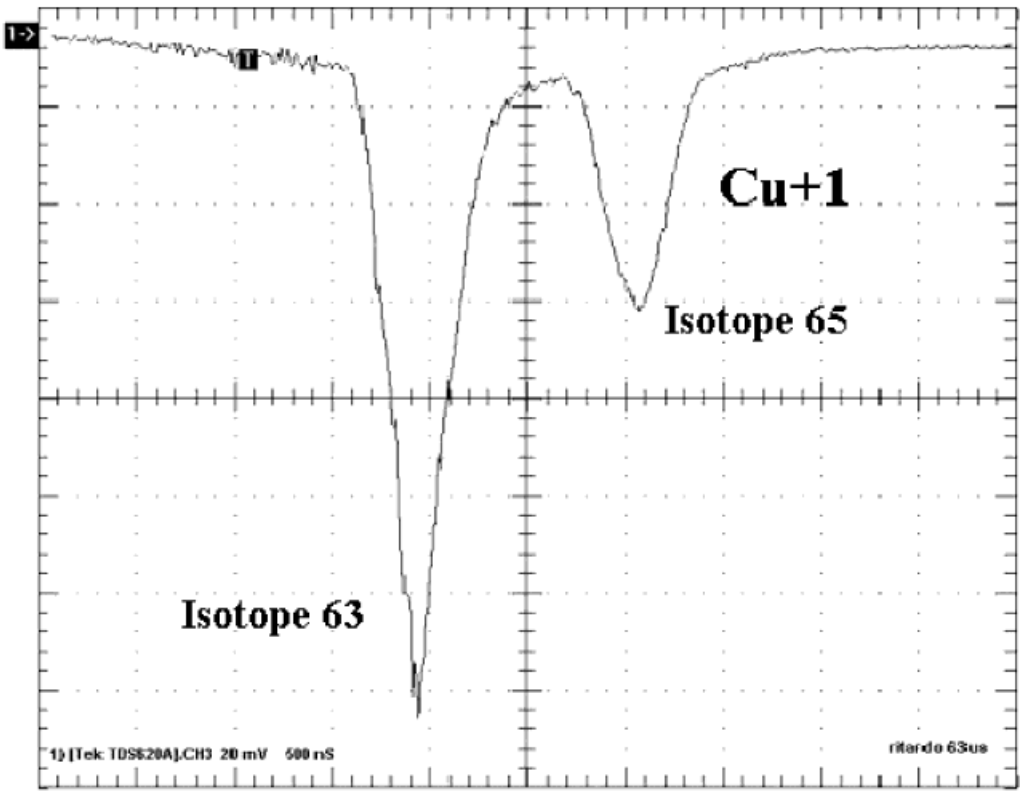

Fig. 8. Waveform of the Cu^{+1} peak displaying the two isotopes ^{63}Cu and ^{65}Cu.

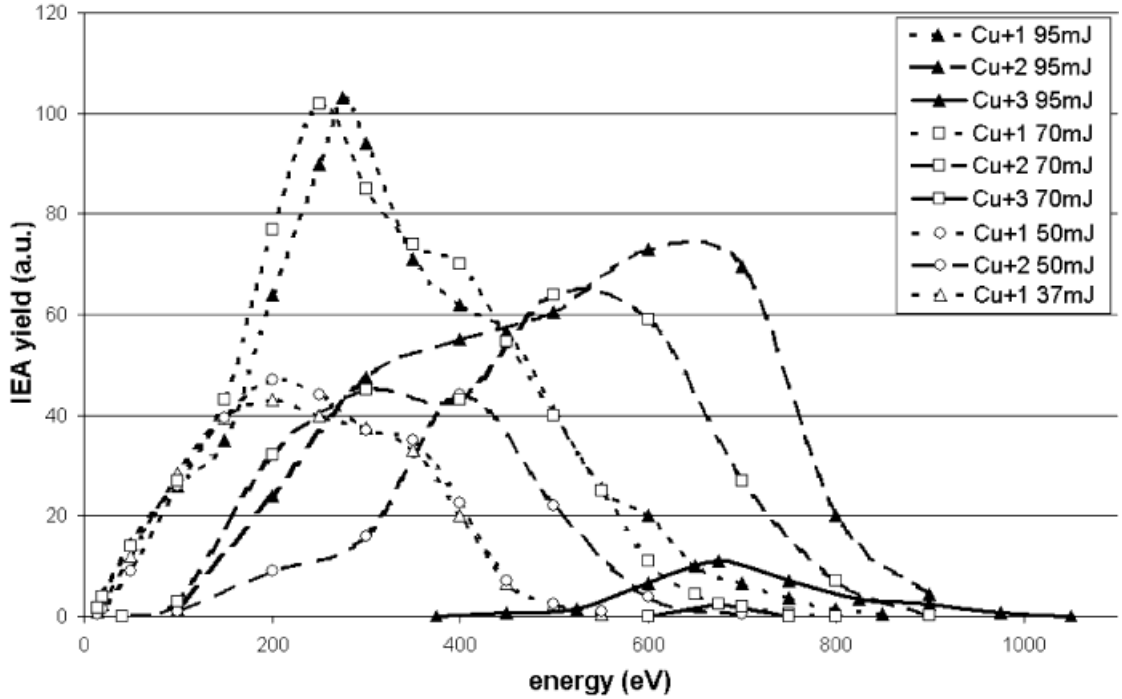

Fig. 9. Ion relative abundance as a function of kinetic energy for different laser energies.

$$I \propto \frac{1}{t^4} \exp\left[-\frac{m}{2kT_{KL}}\left(\frac{x}{t} - v_d\right)^2\right] \tag{4}$$

where I is the WEM current for ions axially revealed, t is the TOF, x is the target-WEM distance, k is the Boltzmann constant, T_{KL} is the Knudsen layer temperature and v_d is the drift velocity. By fitting IEA spectra with Eq. 4, we found plasma temperature and drift velocity values, which are different for each ion distribution. Then ion mean kinetic energy, $\langle E \rangle$, was calculated, according to the following relation:

$$\langle E \rangle = \frac{1}{2} m v_d^2 + \frac{3}{2} kT_{KL}.$$

As an example, we report in Table 1 data concerning Cu^{+1} ion at four laser energies. The temperature values increase as the laser energy decreases, while the drift velocity behavior follows an opposite trend. However, the ion mean kinetic energy increases with the laser energy, as one can expect. This result would indicate that, in our power density range, plasma energy is shared advantaging the tidy collective motion against the untidy thermal one.

2.3. Beam extraction

We performed even preliminary studies about the ion beam extraction from the plasma. For this goal an expansion chamber was necessary in order to avoid arcs between the plasma and ground. In fact, due to the expanding chamber, the plasma expands until the accelerating gap decreasing its density and the probability to get short-circuits. The laser energy used was 70 mJ and the accelerating voltage applied to the target stem was varied up to 16 kV. During these measurements the Faraday cup, with the suppression ring polarized at -100 V respect to the FC bias, was placed at 147 cm from the target along the drift tube. The accelerating gap electrodes have two coaxial holes of 1 cm in diameter for ion extraction. Figure 2 shows a sketch of the accelerating electrodes. Figure 10 shows the cup waveform when an extracting voltage of 16 kV was applied. Different peaks can be distinguished in the TOF spectrum, resulting from the separation of the different ions. The fastest bunches have TOF values compatible with low mass-to-charge ratio and initial kinetic energies of tens of eV. For this reason we believe that these peaks can be due to ions of hydrogen, adsorbed compounds in the target and faster copper. The slowest peak is due to the acceleration of the plasma particles that reach the accelerating gap just after 5 μs and their

Table 1. *Temperature, drift velocity and mean kinetic energy values for Cu^{+1} ions at four laser energies*

Laser energy (mJ)	Temperature (10^5 K)	Drift velocity (10^3 m/s)	Mean energy (eV)
95	3.8	23	230
70	4.3	21	200
50	5.3	14	130
37	7.0	9.6	120

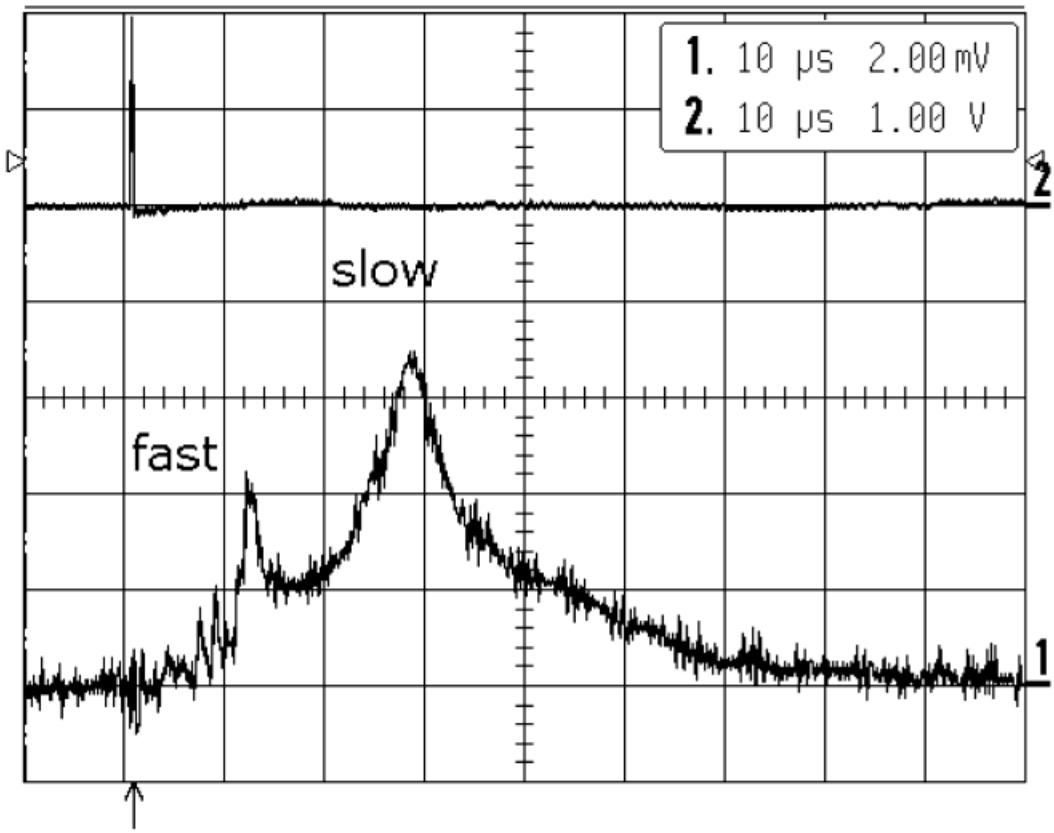

Fig. 10. Trace #1: Faraday cup signal showing the accelerated plasma TOF spectrum obtained with an extracting voltage of 16 kV; trace #2: laser pulse signal recorded by a fast photodiode and used as trigger.

maximum current at 10 μs. Therefore, knowing the plasma particle velocity to be 20 km/s before the acceleration, we expect, with our applied accelerating voltage, an output peak at about 24 μs for Cu^{+1} ions. In fact from Figure 10 one can observe a current peak at 26 μs, very near to the expected value.

ACKNOWLEDGMENTS

The authors are pleased to acknowledge the excellent technical support of Mr. V. Nicolardi and Mr. P. Esposito.

REFERENCES

Anisimov, S. I., Bauerle, D. & Luk'yanchuk, B. S. (1993). *Phy. Rev. B* **48**, 12076–12081.

Ciavola, G. & Gammino, S. (1992). *Rev. Sci. Instrum.* **63**, 2881–2882.

Dubenkov, V. *et al.* (1996). *Laser Part. Beams* **14**(3), 385–392.

Henkelmann *et al*. (1992). *Rev. Sci. Instrum.* **63**, 2828–2830.

Kelly, J. (1990). *J. Chem. Phy.* **92**, 5047–5056.

Kondrashev, S. *et al.* (2000). *Rev. Sci. Instrum.* **71**, 1409–1412.

Kruer, W.L. (1986). Laser-plasma interactions 3 (Hooper, M.B., Ed.), pp. 79–85. SUSSP Publications, Edinburgh.

Làska, L. *et al.* (2000). *Rev. Sci. Instrum.* **71**, 927–930.

Luches, A., Nassisi, V. & Pecoraro, A. (1993). *Appl. Phys. B* **57**, 163–165.

Picardi, L. *et al*. (1994). *Proc. EPAC'94*, 2607–2609.

Sharkov, B. Yu. *et al*. (1998). *Rev. Sci. Instrum.* **69**, 1035–1039.

Sherwood, T.R. (1992). *Rev. Sci. Instrum.* **63**, 2789–2793.

Torrisi, L. *et al.* (2003). *Appl. Surf. Sci*. **210**, 262–273.

Wong, K., Chan, K., Yeung, K.W. & Lau, K.S. (2003). *J. Mater. Process. Technol*. **132**, 114–118.